Hindawi Publishing Corporation
Advances in High Energy Physics
Volume 2013, Article ID 324075, 6 pages
http://dx.doi.org/10.1155/2013/324075

Research Article

On Antiproton Production in 158 GeV/c Proton-Carbon Collisions and Nuclear Temperature of Interacting System

Fu-Hu Liu, Ya-Hui Chen, Ya-Qin Gao, and Hua-Rong Wei

Institute of Theoretical Physics, Shanxi University, Taiyuan, Shanxi 030006, China

Correspondence should be addressed to Fu-Hu Liu; fuhuliu@163.com

Received 28 March 2013; Revised 15 July 2013; Accepted 16 July 2013

Academic Editor: Bhartendu K. Singh

The multisource thermal model is used in this paper to analyze the antiproton ($\overline{p}$) production process in high-energy proton-carbon (p-C) collisions. The transverse momentum, Feynman variable, and rapidity distributions of antiprotons in the nucleon-nucleon center-of-mass system are calculated by using the model. The modeling results are compared and found to be in agreement with the experimental data measured by the NA49 Collaboration at 158 GeV/c beam momentum. As a parameter, the nuclear temperature of interacting system extracted from the antiproton spectrum is estimated to be about 150 MeV.

1. Introduction

High-energy collisions are an important experimental phenomenon in modern physics. From fixed target experiments at accelerators to collider experiments, a lot of experimental results have been reported. In the collisions, an incident projectile and a fixed target (or another incident target at colliders) can be particles, ions, or nuclei. Generally, the products in nucleus-nucleus collisions are more abundant than those in particle-particle collision. The analysis of the former one is also more complex. As a transition stage from particle-particle collision to nucleus-nucleus collisions, particle-nucleus collisions have not only abundant experimental results but also simpler physics process. In fact, in proton induced nuclear collisions, the projectile is simple and has no spectator's contribution, and the target is complex and has spectator's contribution to final state.

Many models have been proposed in the field of high-energy collisions, for example, the equivalent quark-gluon string model [1], the hadron resonance gas model [2, 3], the statistical multifragmentation model [4], the expanding and emitting source model [5] or the expanding-evaporating source model [6], the nonequilibrium-statistical relativistic diffusion model [7], the dual parton model [8, 9], the relativistic or ultrarelativistic quantum molecular dynamics model [10–13], and so forth. In a workshop [14] held a few years ago at the CERN Theory Institute, more models have reported their predictions for the collision program at the LHC energies. Most of the mentioned models are microscopic models based on quantum chromodynamics (QCD) and concern the system evolution and dynamical process. Parts of them are thermal and statistical models and focus on the global properties of interacting system and final-state products.

In the past years, we have proposed a multisource thermal model [15, 16] and extended it to relativistic situation [17] for descriptions of particle production in high-energy collisions. Some experimental results are described by the model. Recently, the NA49 Collaboration reported inclusive productions in proton-carbon (p-C) collisions at 158 GeV/c beam momentum [18]. We are interested in the description of antiproton ($\overline{p}$) production and will give a description in this paper. Because there is no effect of leading particles, the distribution law of antiprotons in analysis is simpler than that of protons.

2. The Model

According to the multisource thermal model [15–17], many emission sources are formed in high-energy collisions. In the rapidity space, most of these sources are distributed

homogeneously in a projectile cylinder and a target cylinder due to the penetration of the projectile and the target. In the rapidity space, the projectile and target cylinders are located in the rapidity intervals $[y_{P_{\min}}, y_{P_{\max}}]$ and $[y_{T_{\min}}, y_{T_{\max}}]$, respectively. For antiproton production in proton-carbon collisions, the leading nucleons have no contribution, but the target spectator contributes a cylinder in the rapidity interval $[y_{\mathrm{TS}_{\min}}, y_{\mathrm{TS}_{\max}}]$ due to the produced particles causing the cascade collisions in the spectator. Let K_{TS} denote the weight of the target spectator cylinder; the weights of the projectile and target cylinders are the same: $(1 - K_{\mathrm{TS}})/2$.

We define the beam direction to be the *oz* axis and the reaction plane to be the *xoz* plane. In the source rest frame, let T' and p' denote the source temperature and particle momentum, respectively. Considering the relativistic effect [19, 20], we have the p' distribution in the relativistic ideal gas model to be

$$f_{p'}\left(p'\right) = \frac{1}{N}\frac{dN}{dp'} = Cp'^2 \exp\left(-\frac{\sqrt{p'^2 + m_0^2}}{kT'}\right), \quad (1)$$

where k denotes the Boltzmann constant, m_0 denotes the rest mass of the considered particle, $C = 1/(m_0^2 kT') \cdot 1/(K_2(m_0/kT'))$ is the normalization constant, and $K_2(m_0/kT')$ is the modified Bessel function of order 2. In the previous equation, we have taken the natural system of units in which the speed c of light in vacuum is 1.

In the Monte Carlo method, p' can be obtained by solving the inequality $|\int_0^{p'} f_{p'}(p')dp' - R_1 \le O|$, where R_1 and O are a random number distributed evenly in the range from 0 to 1 where 0 and 1 are included (i.e., in $[0, 1]$) and a small quantity, respectively. Let θ' denote the emission angle of the considered particle. An isotropic emission gives $\theta' = \arccos(1-2R_2)$, where R_2 is another random number in $[0, 1]$. Then, the particle transverse momentum $p'_T \equiv p' \sin\theta'$, longitudinal momentum $p'_L \equiv p' \cos\theta'$, transverse mass $m'_T \equiv \sqrt{p'^2_T + m_0^2}$, energy $E' \equiv \sqrt{p'^2 + m_0^2}$, kinetic energy $E'_K \equiv E' - m_0$, and rapidity $y' \equiv 0.5\ln[(E' + p'_L)/(E' - p'_L)]$ can be obtained. Particularly [17], the distributions of p'_T, p'_L, and m'_T are

$$f_{p'_T}\left(p'_T\right) = \frac{1}{N}\frac{dN}{dp'_T} = C_1 p'_T \exp\left(-\frac{\sqrt{p'^2_T + m_0^2}}{kT'}\right), \quad (2)$$

$$f_{p'_L}\left(p'_L\right) = \frac{1}{N}\frac{dN}{dp'_L} = C_2\sqrt{p'^2_L + m_0^2}\exp\left(-\frac{\sqrt{p'^2_L + m_0^2}}{kT'}\right), \quad (3)$$

$$f_{m'_T}\left(m'_T\right) = \frac{1}{N}\frac{dN}{dm'_T} = C_1 m'_T \exp\left(-\frac{m'_T}{kT'}\right), \quad (4)$$

respectively, where C_1 and C_2 are the normalization constants. We would like to point out that (2) is in fact the Boltzmann distribution which is used in the literature (e.g., [21]). Both (2) and (3) are valid because they are in agreement with the Monte Carlo calculations based on the definitions. The distributions of E' and E'_K are

$$f_{E'}\left(E'\right) = \frac{1}{N}\frac{dN}{dE'} = CE'\sqrt{E'^2 - m_0^2}\exp\left(-\frac{E'}{kT'}\right), \quad (5)$$

$$\begin{aligned} f_{E'_K}\left(E'_K\right) &= \frac{1}{N}\frac{dN}{dE'_K} \\ &= C\left(E'_K + m_0\right) \\ &\quad \times \sqrt{\left(E'_K + m_0\right)^2 - m_0^2}\exp\left(-\frac{E'_K + m_0}{kT'}\right), \end{aligned} \quad (6)$$

respectively. The distribution of velocity v' is

$$f_{v'}\left(v'\right) = \frac{1}{N}\frac{dN}{dv'} = C\frac{m_0^3 v'^2}{\left(1 - v'^2\right)^{5/2}}\exp\left(-\frac{m_0}{kT'\sqrt{1 - v'^2}}\right). \quad (7)$$

In the nucleon-nucleon center-of-mass system, let y_x denote the source rapidity. According to different weights, we have $y_x = (y_{P_{\max}} - y_{P_{\min}})R_3 + y_{P_{\min}}$ for the projectile cylinder, $y_x = (y_{T_{\max}} - y_{T_{\min}})R_4 + y_{T_{\min}}$ for the target cylinder, or $y_x = (y_{\mathrm{TS}_{\max}} - y_{\mathrm{TS}_{\min}})R_5 + y_{\mathrm{TS}_{\min}}$ for the target spectator cylinders, where R_3, R_4, and R_5 are random variables in $[0, 1]$. Then, the particle rapidity $y = y_x + y'$, transverse momentum $p_T = p'_T$, longitudinal momentum $p_L = p'_L \cosh y + E' \sinh y$, momentum $p = \sqrt{p_T^2 + p_L^2}$, energy $E = \sqrt{p^2 + m_0^2}$, transverse mass $m_T = m'_T$, and Feynman variable $x_F = 2p_L/\sqrt{s}$ can be obtained, where $\sqrt{s}$ is the energy in the center-of-mass system. Then, we transform all of the concerned kinetic quantities from the rest frame of a single source to the nucleon-nucleon center-of-mass system. The effects of the multiple sources are obtained by different y_x. On the other hand, from the definition of Feynman variable, we have $p_L = 0.5x_F\sqrt{s}$. Then, $p = \sqrt{p_T^2 + (0.5x_F\sqrt{s})^2}$, $E = \sqrt{p_T^2 + (0.5x_F\sqrt{s})^2 + m_0^2}$, and $y = 0.5\ln[(E + p_L)/(E - p_L)] = 0.5\ln[(\sqrt{p_T^2 + (0.5x_F\sqrt{s})^2 + m_0^2} + 0.5x_F\sqrt{s})/(\sqrt{p_T^2 + (0.5x_F\sqrt{s})^2 + m_0^2}) - 0.5x_F\sqrt{s}]$ are the functions of x_F. Particularly, the relationship between y and x_F at a given p_T is built.

3. Comparison with Experimental Data

Figure 1 shows the invariant cross-section, $f(x_F, p_T)$, in the units of mb/(GeV$^2/c^3$) for $\overline{p}$ produced in p-C collisions at 158 GeV/c beam momentum. The distributions of p_T, $f(x_F, p_T) \propto (1/N)(dN/p_T dp_T)$, at different x_F are given. The symbols represent the experimental data of the NA49 Collaboration [18], and the curves are our results calculated by the multisource thermal model [15–17]. To show a clear representation, the values of $f(x_F, p_T)$ at different x_F are scaled by multiplying constants shown in the figure. In

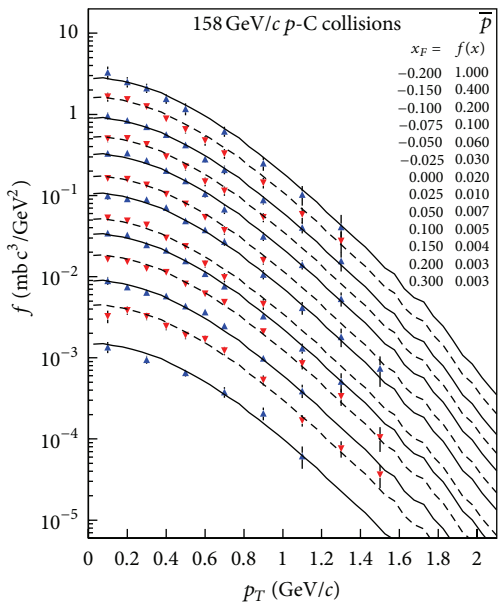

FIGURE 1: Transverse momentum distributions of antiprotons in p-C collisions at 158 GeV/c. The symbols represent the experimental data of the NA49 Collaboration [18] at different x_F, and the curves are our results calculated by the multisource thermal model.

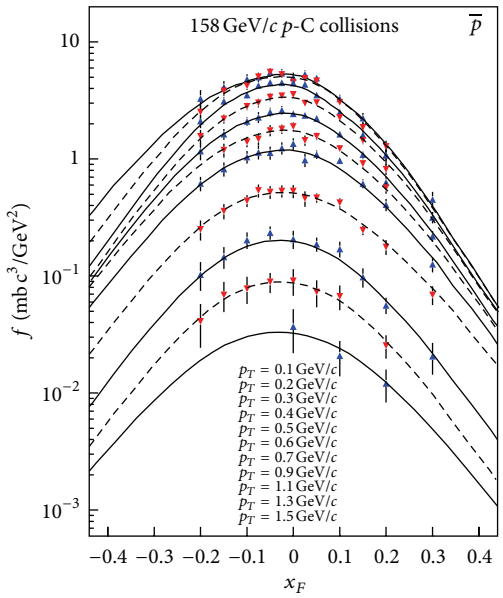

FIGURE 2: Feynman variable distributions of antiprotons in p-C collisions at 158 GeV/c. The symbols represent the experimental data of the NA49 Collaboration [18] at different p_T, and the curves are our results calculated by the multisource thermal model.

the calculation, we have used the method of χ^2 testing to determine the parameter values. The value of the only free parameter is $kT' = (150 \pm 10)$ MeV for different x_F values and with the values of χ^2 per degree of freedom (χ^2/dof) is in the order 0.759, 1.042, 0.564, 0.888, 0.699, 0.994, 0.436, 1.348, 0.895, 0.552, 0.298, 0.424, and 0.450, respectively. One can see that the model describes well the experimental data.

The distributions of x_F and y at different p_T for $\overline{p}$ produced in p-C collisions at 158 GeV/c are presented in Figures 2 and 3, respectively. The symbols represent the experimental data of the NA49 Collaboration [18] and the curves are our calculated results. The value of kT' is the same as that for Figure 1 and $K_{\mathrm{TS}} = 0.15 \pm 0.01$. The values of other parameters (rapidity shifts) which have a relative error of 6% are given in Table 1 with the values of χ^2/dof. Once again the model describes well the experimental data.

To see the dependences of different rapidity shifts on p_T, the relations of $y_{P_{\max}} - p_T$, $y_{P_{\min}} - p_T$, $y_{T_{\max}} - p_T$, $y_{T_{\min}} - p_T$, $y_{\mathrm{TS}_{\max}} - p_T$, and $y_{\mathrm{TS}_{\min}} - p_T$ are given in Figure 4. The symbols represent the parameter values used in Figures 2 and 3. The lines are our fitted results described by the equations $y_X = ap_T + b$, where y_X denotes different rapidity shifts and the values of a and b are given in Table 2 with the values of χ^2/dof. One can see that $y_{P_{\max}}$ decreases and $y_{T_{\min}}$ and $y_{\mathrm{TS}_{\min}}$ increase with the increases of p_T. A very slight decrease in $y_{T_{\max}}$ and very slight increases in $y_{T_{\min}}$ and $y_{\mathrm{TS}_{\min}}$ are observed with the increase of p_T. If we define $y_{P_{\max}} - y_{T_{\min}}$ as the total length of the projectile and target cylinders, this length shows a decrease with the increase of p_T. The condition $y_{P_{\max}} - y_{T_{\min}} = 0$ results in a zero length cylinder which gives approximately the maximum p_T to be 3.82 GeV/c. From $p_T = 2$ GeV/c to 3.82 GeV/c, the relations of $y_{P_{\min}} - p_T$, $y_{T_{\max}} - p_T$, and $y_{\mathrm{TS}_{\max}} - p_T$

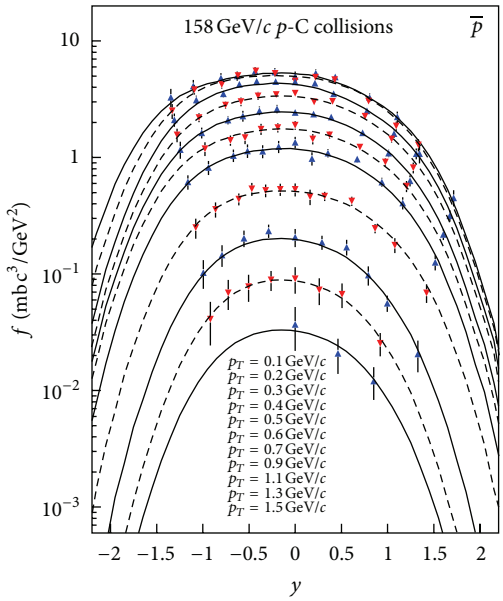

FIGURE 3: Rapidity distributions of antiprotons in p-C collisions at 158 GeV/c. The symbols represent the experimental data of the NA49 Collaboration [18] at different p_T, and the curves are our results calculated by the multisource thermal model.

will not be the same linear changes as those in the region of $p_T < 2$ GeV/c. The projectile and target cylinders will be from partly overlapping to totally overlapping. The length will become in fact shorter and shorter and finally will be a single source.

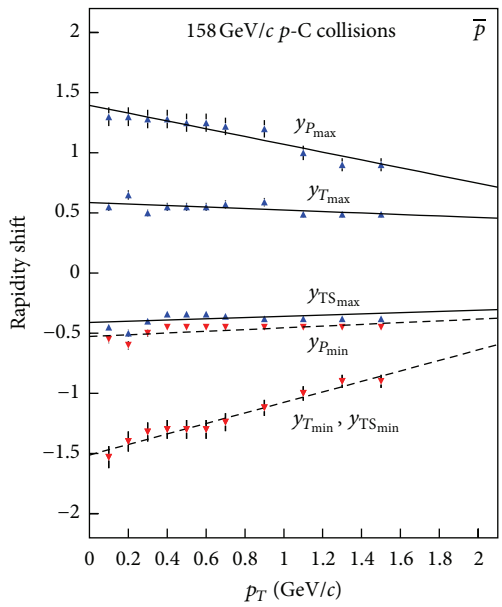

FIGURE 4: Correlations between the rapidity shifts and p_T. The symbols represent the parameter values used in Figures 2 and 3 due to the experimental data of the NA49 Collaboration [18], and the lines are our fitted results.

4. Discussions

In the previous discussions, we have assumed in fact that a thermal equilibrium (or a local thermal equilibrium) is achieved in the collisions when the thermal source freezes out final-state particles. Thus, the concept of temperature can be used in our calculation. In the calculation, we have not given special attention to the possible presence of early emitting source before an achievement of equilibrium. In fact, when studying antiprotons instead of protons with leading particle contributions, the preequilibrium emissions are naturally excluded. This is the reason that we have not studied protons but antiprotons.

In high-energy collisions, the most abundantly produced particles are pions. The produced processes of pions, kaons, and other particles are more complex than those of antiprotons and protons. If we use the relativistic ideal gas model [19, 20] or other models [1–14] to describe a single source, in the case of considering properly the number, contribution, position, and arrangement of the multiple sources, many particle spectra can be described by the multisource thermal model [15, 16] or hybrid multisource model. The hybrid multisource model means that we can use a multicomponent distribution to describe particle spectra, and the single component distribution is just obtained from some available models [1–14]. As an example, we have analyzed only the antiproton spectra in the present work. In fact, these models [1–16] describe experimental data of different particles in different collisions at different energies.

In a previous work [21], the transverse momentum and rapidity distributions of ϕ mesons produced in Pb-Pb collisions at 20A, 30A, 40A, 80A, and 158A GeV were studied by using the multisource thermal model (or multisource ideal gas model). In another previous work [22], the transverse mass distributions of protons produced in Au-Au collisions at 8A GeV and Pb-Pb collisions at 158A GeV were studied by using the same or similar model. Besides, the transverse mass spectra of protons, pions, kaons, Lambdas, and Antilambdas produced in Au-Au collisions at 2A, 4A, 6A, and 8A GeV and Pb-Pb collisions at 20A, 30A, 40A, 80A, and 158A GeV were studied [23]. The pseudorapidity distributions of charged particles produced in p-$\overline{p}$ collisions at 0.053, 0.2, 0.54, 0.546, 0.63, 0.9, and 1.8 TeV; the pseudorapidity and multiplicity distributions of charged particles produced in p-p collisions at 0.9, 2.36, and 7 GeV; and the pseudorapidity distributions of charged particles produced in Pb-Pb collisions at 2.76A TeV were studied too [24–27]. We would like to say that the multisource thermal model used in the present work describes different particles produced in different collisions at different energies. However, the present work is the first one to describe the antiproton production by the model.

We would like to point out that the temperature extracted in the present work reflects excitation degree of thermal source when it freezes out antiprotons. According to production process, the source temperature extracted from proton spectrum is on average less than 150 MeV due to some protons being leading particles and that from meson spectrum is higher than 150 MeV due to violent collisions. If we exclude the contributions of leading particles, the temperature extracted from proton spectrum is approximately equal to 150 MeV. These results are consistent with other measurements in the field [18] and with other model expectations [14].

The target spectator weighting factor is found to be about 15%. This reflects the contribution of cascade collisions in the target spectator caused by the produced particles. In high-energy collisions, the spectator effect cannot be neglected in most cases. Particularly, in asymmetric collisions such as proton-carbon collisions, one can obtain some asymmetric rapidity spectra. The contribution of target spectators has to be considered. In nucleus-nucleus collisions, both the contributions of projectile and target spectators have to be considered.

5. Conclusions

We have analyzed the transverse momentum, Feynman variable, and rapidity distributions of antiprotons produced in proton-carbon collisions at high-energy by using the multisource thermal model. This model assumes that many sources are formed in high energy collisions. Each source is treated as a relativistic ideal gas. The distributions of momenta, transverse momenta, longitudinal momenta, energies, kinetic energies, transverse mass, velocities, and other related quantities for a given kind of particles at a given temperature in the source rest frame can be obtained.

In the comparisons with the experimental data, the transverse momentum distribution is not related to the source positions and arrangements but to the temperature of the rest source. A single-temperature distribution describes the

Table 1: Values of the rapidity shifts and χ^2/dof for the fits in Figures 2 and 3. The relative errors of the rapidity shifts are 6%.

p_T(GeV/c)	$y_{P_{\max}}$	$y_{P_{\min}}$	$y_{T_{\max}}$	$y_{T_{\min}}$	$y_{\mathrm{TS}_{\max}}$	$y_{\mathrm{TS}_{\min}}$	χ^2/dof (Figure 2)	χ^2/dof (Figure 3)
0.1	1.30	−0.55	0.55	−1.52	−0.45	−1.53	0.298	0.603
0.2	1.30	−0.60	0.65	−1.40	−0.50	−1.40	0.719	0.651
0.3	1.28	−0.50	0.50	−1.32	−0.40	−1.32	0.595	0.438
0.4	1.28	−0.45	0.55	−1.30	−0.34	−1.30	0.552	0.501
0.5	1.25	−0.45	0.55	−1.30	−0.34	−1.30	0.425	0.703
0.6	1.25	−0.45	0.55	−1.30	−0.34	−1.30	0.340	0.320
0.7	1.22	−0.45	0.57	−1.24	−0.36	−1.24	0.143	0.586
0.9	1.20	−0.45	0.59	−1.12	−0.38	−1.12	0.207	0.460
1.1	1.00	−0.45	0.49	−1.00	−0.38	−1.00	1.166	1.867
1.3	0.90	−0.45	0.49	−0.90	−0.38	−0.90	0.570[a]	0.570[a]
1.5	0.90	−0.45	0.49	−0.90	−0.38	−0.90	0.125[a]	0.371[a]

[a]The value of χ^2 is given instead of χ^2/dof.

Table 2: Values of a and b in equations $y_X = ap_T + b$. The unit of p_T is GeV/c.

y_X	a [(GeV/c) $^{-1}$]	b	χ^2/dof
$y_{P_{\max}}$	−0.324 ± 0.038	1.395 ± 0.031	0.040
$y_{P_{\min}}$	0.072 ± 0.029	−0.527 ± 0.024	0.115
$y_{T_{\max}}$	−0.062 ± 0.030	0.586 ± 0.024	0.098
$y_{T_{\min}}$	0.437 ± 0.031	−1.512 ± 0.025	0.024
$y_{\mathrm{TS}_{\max}}$	0.040 ± 0.033	−0.414 ± 0.027	0.242
$y_{\mathrm{TS}_{\min}}$	0.437 ± 0.031	−1.512 ± 0.025	0.024

transverse momentum distributions of antiprotons produced in proton-carbon collisions at 158 GeV/c measured by the NA49 Collaboration [18]. From the transverse momentum distributions of antiprotons, we determine that the source temperature is approximately 150 MeV.

In longitudinal distributions, the distributions of Feynman variables and rapidities are mainly related to the source positions and arrangements. In rapidity space, these sources form a projectile cylinder and a target cylinder. Particularly, in proton-carbon collisions, a target spectator cylinder consisting of a series of sources has a weight for the production of antiprotons. By using the three cylinders, the model describes the distributions of Feynman variables and rapidities for antiprotons in proton-carbon collisions at high energy. Our analyses show that the weight of the target spectator cylinder is 15%. Both the weights of the projectile cylinder and the target cylinder are the same.

With the increase of the transverse momentum, the maximum rapidity shift of the projectile cylinder has a decrease, the minimum rapidity shifts of the target and target spectator cylinders have increases, the maximum rapidity shift of the target cylinder has a very slight decrease, and the minimum rapidity shift of the projectile cylinder and the maximum rapidity shift of the target spectator cylinder have very slight increases. The length of the total projectile and target cylinders decreases with the increase of the transverse momentum.

Combined with the previous works [15, 16, 21–27] analyzed by the multisource thermal model, we guess the energy behavior of some parameters of the model here. For a given projectile-target impacting system, the rapidity shifts of the cylinders increase slowly with the logarithmic center-of-mass energy and do not depend obviously on the centrality. The temperatures extracted from the hadron spectra increase slowly with the energy and centrality. The relative contributions of the cylinders, leading nucleons, and spectators have no obvious relation to the energy but the centrality. In central collisions, the leading nucleons and spectators have very limited contributions or no contribution to the final-state distributions; and in peripheral collisions, they have large contributions.

Acknowledgments

This work was supported by the National Natural Science Foundation of China under Grant no. 10975095, the China National Fundamental Fund of Personnel Training under Grant no. J1103210, the Open Research Subject of the Chinese Academy of Sciences Large-Scale Scientific Facility under Grant no. 2060205, and the Shanxi Scholarship Council of China.

References

[1] A. B. Kaidalov, "The quark-gluon structure of the pomeron and the rise of inclusive spectra at high energies," *Physics Letters B*, vol. 116, no. 6, pp. 459–463, 1982.

[2] F. Karsch, K. Redlich, and A. Tawfik, "Thermodynamics at non-zero baryon number density: a comparison of lattice and hadron resonance gas model calculations," *Physics Letters B*, vol. 571, no. 1-2, pp. 67–74, 2003.

[3] F. Karsch, K. Redlich, and A. Tawfik, "Hadron resonance mass spectrum and lattice QCD thermodynamics," *European Physical Journal C*, vol. 29, no. 4, pp. 549–556, 2003.

[4] J. P. Bondorf, A. S. Botvina, A. S. Iljinov, I. N. Mishustin, and K. Sneppen, "Statistical multifragmentation of nuclei," *Physics Report*, vol. 257, no. 3, pp. 133–221, 1995.

[5] W. A. Friedman, "Basis for a characteristic temperature in nuclear fragmentation," *Physical Review Letters*, vol. 60, no. 21, pp. 2125–2128, 1988.

[6] W. A. Friedman, "Rapid massive cluster formation," *Physical Review C*, vol. 42, no. 2, pp. 667–673, 1990.

[7] G. Wolschin, "Pseudorapidity distributions of produced charged hadrons in pp collisions at RHIC and LHC energies," *Europhysics Letters*, vol. 95, no. 6, Article ID 61001, 6 pages, 2011.

[8] A. Capella, J. Kwieciński, and J. Tran Thanh Van, "High-energy nucleus-nucleus inelastic interactions in the dual parton model," *Physics Letters B*, vol. 108, no. 4-5, pp. 347–350, 1982.

[9] A. Capella, U. Sukhatme, C.-I. Tan, and J. Tran Thanh Van, "Dual parton model," *Physics Report*, vol. 236, no. 4-5, pp. 225–329, 1994.

[10] J. Aichelin, G. Peilert, A. Bohnet, A. Rosenhauer, H. Stöcker, and W. Greiner, "Quantum molecular dynamics approach to heavy ion collisions: description of the model, comparison with fragmentation data, and the mechanism of fragment formation," *Physical Review C*, vol. 37, no. 6, pp. 2451–2468, 1988.

[11] G. Peilert, H. Stöcker, W. Greiner, A. Rosenhauer, A. Bohnet, and J. Aichelin, "Multifragmentation, fragment flow, and the nuclear equation of state," *Physical Review C*, vol. 39, no. 4, pp. 1402–1419, 1989.

[12] S. A. Bass, H. Weber, C. Ernst et al., "Reaction dynamics in Pb + Pb at the CERN/SPS: from partonic degrees of freedom to freeze-out," *Progress in Particle and Nuclear Physics*, vol. 42, pp. 313–322, 1999.

[13] M. Bleicher, E. Zabrodin, C. Spieles et al., "Relativistic hadron-hadron collisions in the ultra-relativistic quantum molecular dynamics model," *Journal of Physics G*, vol. 25, no. 9, pp. 1859–1896, 1999.

[14] S. Abreu et al., "Heavy-ion collisions at the LHC—last call for predictions," *Journal of Physics G*, vol. 35, no. 5, Article ID 054001, 170 pages, 2008.

[15] F.-H. Liu, "Longitudinal and transverse flows of protons in 2-8 A GeV Au-Au collisions," *Europhysics Letters*, vol. 63, no. 2, pp. 193–199, 2003.

[16] F.-H. Liu, N. N. A. Allah, and B. K. Singh, "Dependence of black fragment azimuthal and projected angular distributions on polar angle in silicon-emulsion collisions at 4.5A GeV/c," *Physical Review C*, vol. 69, no. 5, Article ID 057601, 4 pages, 2004.

[17] F. H. Liu, C. X. Tian, M. Y. Duan, and B. C. Li, "Relativistic and quantum revisions of the multisource thermal model in high-energy collisions," *Advances in High Energy Physics*, vol. 2012, Article ID 287521, 9 pages, 2012.

[18] B. Baatar, G. Barr, J. Bartke et al., "Inclusive production of protons, anti-protons, neutrons, deuterons and tritons in p+C collisions at 158 Gev/c beam momentum," *European Physical Journal C*, vol. 73, pp. 2364–2429, 2013.

[19] J. L. Synge, *The Relativistic Gas*, North-Holland, Amsterdam, The Netherlands, 1957.

[20] C. D. Dermer, "The production spectrum of a relativistic Maxwell-Boltzmann gas," *The Astrophysical Journal*, vol. 280, no. 1, pp. 328–333, 1984.

[21] C.-R. Meng, "Transverse momentum and rapidity distributions of φ mesons produced in Pb-Pb collisions at SPS energies," *Chinese Physics Letters*, vol. 26, no. 10, Article ID 102501, 4 pages, 2009.

[22] W.-J. Xie, "Transverse mass distributions of protons produced in heavy-ion collisions at high energies," *Chinese Physics C*, vol. 34, no. 11, pp. 1717–1723, 2010.

[23] W.-J. Xie, D. Yang, C.-P. Wang, and Z.-G. Wang, "Transverse mass distributions in central heavy-ion collisions at high energies," *Chinese Physics C*, vol. 35, no. 4, pp. 355–362, 2011.

[24] J.-X. Sun, F.-H. Liu, E.-Q. Wang, Y. Sun, and Z. Sun, "Pseudorapidity distributions of charged particles in p-$\overline{p}$ or p-p collisions at high energies and predictions at ultrahigh energies," *Physical Review C*, vol. 83, no. 1, Article ID 014001, 7 pages, 2011.

[25] J. X. Sun, L. L. Liu, E. Q. Wang, and F. H. Liu, "Charged particle pseudorapidity distribution in high energy or collisions and the improved multi-source thermal model," *Indian Journal of Physics*, vol. 87, no. 2, pp. 177–184, 2013.

[26] J. M. Feng, C. X. Tian, R. F. Si, and F. H. Liu, "Multiple particle production in proton-proton collisions at energies available at the Large Hadron Collider," *Journal of the Korean Physical Society*, vol. 61, no. 4, pp. 518–522, 2012.

[27] J. X. Sun, C. X. Tian, E. Q. Wang, and F. H. Liu, "Dependence of charged particle pseudorapidity distributions on centrality in Pb-Pb collisions at $\sqrt{S_{NN}}$=2. 76 TeV," *Chinese Physics Letters*, vol. 30, no. 2, Article ID 022501, 4 pages, 2013.